



# Observation of gain spiking of optical frequency comb in a microcavity

YUANLIN ZHENG,<sup>1</sup> TIAN QIN,<sup>2</sup> JIANFAN YANG,<sup>2</sup> XIANFENG CHEN,<sup>1,4</sup> LI GE,<sup>3,5</sup> AND WENJIE WAN<sup>1,2,\*</sup>

<sup>1</sup>The State Key Laboratory of Advanced Optical Communication Systems and Networks, School of Physics and Astronomy, Shanghai Jiao Tong University, Shanghai 200240, China

<sup>2</sup>The University of Michigan-Shanghai Jiao Tong University Joint Institute, MOE Key Laboratory for Laser Plasmas and Collaborative Innovation Center of IFSA, Shanghai Jiao Tong University, Shanghai 200240, China

<sup>3</sup>Department of Engineering Science and Physics, College of Staten Island, the City University of New York, NY 10314, and the Graduate Center, CUNY, New York, NY 10016, USA

<sup>4</sup>xfchen@sjtu.edu.cn

<sup>5</sup>li.ge@csi.cuny.edu

\*wenjie.wan@sjtu.edu.cn

**Abstract:** Optical frequency combs are crucial for both fundamental science and applications that demand a wide frequency range and ultra-high resolution. Recent advances in optical frequency combs based on the nonlinear Kerr effect in microcavities have opened up new opportunities with such compact platforms. Although optical frequency combs have previously been well studied in the steady state, some fundamental perspectives such as nonlinear phase modulation during comb generations are yet explored. Here we demonstrate transient nonlinear dynamics during the formation of optical frequency combs inside a Kerr microcavity. We show that gain spiking forms due to nonlinear phase modulation causing comb lines' self-detuning from nearby cavity resonances, which provides one key mechanism to stabilize optical frequency combs. Moreover, we have observed nonlinear beating by injecting an external probe to examine nonlinear cross-phase modulation between comb lines. These nonlinear dynamics reveal the hidden features of self-stabilization and cross modulation during transient comb generations, which may enable new applications in mode-locking comb and tunable comb generation in microcavities.

© 2017 Optical Society of America under the terms of the [OSA Open Access Publishing Agreement](#)

**OCIS codes:** (140.3945) Microcavities; (190.4380) Nonlinear optics, four-wave mixing; (190.3270) Kerr effect.

## References and links

1. T. Udem, R. Holzwarth, and T. W. Hänsch, "Optical frequency metrology," *Nature* **416**(6877), 233–237 (2002).
2. S. A. Diddams, L. Hollberg, and V. Mbele, "Molecular fingerprinting with the resolved modes of a femtosecond laser frequency comb," *Nature* **445**(7128), 627–630 (2007).
3. T. M. Fortier, M. S. Kirchner, F. Quinlan, J. Taylor, J. C. Bergquist, T. Rosenband, N. Lemke, A. Ludlow, Y. Jiang, C. W. Oates, and S. A. Diddams, "Generation of ultrastable microwaves via optical frequency division," *Nat. Photonics* **5**, 425–429 (2011).
4. A. A. Savchenkov, A. B. Matsko, V. S. Ilchenko, I. Solomatine, D. Seidel, and L. Maleki, "Tunable optical frequency comb with a crystalline whispering gallery mode resonator," *Phys. Rev. Lett.* **101**(9), 093902 (2008).
5. S. B. Papp, K. Beha, P. Del'Haye, F. Quinlan, H. Lee, K. J. Vahala, and A. S. Diddams, "Microresonator frequency comb optical clock," *Optica* **1**, 10–14 (2014).
6. T. J. Kippenberg, R. Holzwarth, and S. A. Diddams, "Microresonator-based optical frequency combs," *Science* **332**(6029), 555–559 (2011).
7. P. Del'Haye, A. Schliesser, O. Arcizet, T. Wilken, R. Holzwarth, and T. J. Kippenberg, "Optical frequency comb generation from a monolithic microresonator," *Nature* **450**(7173), 1214–1217 (2007).
8. P. Del'Haye, O. Arcizet, A. Schliesser, R. Holzwarth, and T. J. Kippenberg, "Full stabilization of a microresonator-based optical frequency comb," *Phys. Rev. Lett.* **101**(5), 053903 (2008).
9. T. J. Kippenberg, S. M. Spillane, and K. J. Vahala, "Kerr-nonlinearity optical parametric oscillation in an ultrahigh-Q toroid microcavity," *Phys. Rev. Lett.* **93**(8), 083904 (2004).
10. S. M. Spillane, T. J. Kippenberg, and K. J. Vahala, "Ultralow-threshold Raman laser using a spherical dielectric microcavity," *Nature* **415**(6872), 621–623 (2002).

11. X. Yang, Ş. K. Özdemir, B. Peng, H. Yilmaz, F.-C. Lei, G.-L. Long, and L. Yang, "Raman gain induced mode evolution and on-demand coupling control in whispering-gallery-mode microcavities," *Opt. Express* **23**(23), 29573–29583 (2015).
12. J. Kim, M. C. Kuzyk, K. Han, H. Wang, and G. Bahl, "Non-reciprocal Brillouin scattering induced transparency," *Nat. Phys.* **11**, 275–280 (2015).
13. C. Dong, V. Fiore, M. C. Kuzyk, and H. Wang, "Optomechanical dark mode," *Science* **338**(6114), 1609–1613 (2012).
14. D. Kip, M. Soljacic, M. Segev, E. Eugenieva, and D. N. Christodoulides, "Modulation instability and pattern formation in spatially incoherent light beams," *Science* **290**(5491), 495–498 (2000).
15. Z. Chen, M. Mitchell, M. Segev, T. H. Coskun, and D. N. Christodoulides, "Self-trapping of dark incoherent light beams," *Science* **280**(5365), 889–892 (1998).
16. Z. Chen, M. Segev, and D. N. Christodoulides, "Optical spatial solitons: historical overview and recent advances," *Rep. Prog. Phys.* **75**(8), 086401 (2012).
17. T. Herr, V. Brasch, J. D. Jost, C. Y. Wang, N. M. Kondratiev, M. L. Gorodetsky, and T. J. Kippenberg, "Temporal solitons in optical microresonators," *Nat. Photonics* **8**, 145–152 (2014).
18. X. Xue, Y. Xuan, Y. Liu, P.-H. Wang, S. Chen, J. Wang, D. E. Leaird, M. Qi, and A. M. Weiner, "Mode-locked dark pulse Kerr combs in normal-dispersion microresonators," *Nat. Photonics* **9**, 594–600 (2015).
19. A. E. Siegman, *Lasers* (University Science Books, 1986).
20. F. Ferdous, H. Miao, D. E. Leaird, K. Srinivasan, J. Wang, L. Chen, L. T. Varghese, and A. M. Weiner, "Spectral line-by-line pulse shaping of on-chip microresonator frequency combs," *Nat. Photonics* **5**, 770–776 (2011).
21. R. W. Boyd, *Nonlinear optics*, Third Edition (Academic Press, 2008).
22. V. S. Ilchenko, A. A. Savchenkov, A. B. Matsko, and L. Maleki, "Nonlinear optics and crystalline whispering gallery mode cavities," *Phys. Rev. Lett.* **92**(4), 043903 (2004).
23. T. Carmon, L. Yang, and K. Vahala, "Dynamical thermal behavior and thermal self-stability of microcavities," *Opt. Express* **12**(20), 4742–4750 (2004).
24. X. Yi, Q.-F. Yang, K. Youl Yang, and K. Vahala, "Active capture and stabilization of temporal solitons in microresonators," *Opt. Lett.* **41**(9), 2037–2040 (2016).
25. P. Del'Haye, T. Herr, E. Gavartin, M. L. Gorodetsky, R. Holzwarth, and T. J. Kippenberg, "Octave spanning tunable frequency comb from a microresonator," *Phys. Rev. Lett.* **107**(6), 063901 (2011).
26. T. Herr, K. Hartinger, J. Riemensberger, C. Y. Wang, E. Gavartin, R. Holzwarth, M. L. Gorodetsky, and T. J. Kippenberg, "Universal formation dynamics and noise of Kerr-frequency combs in microresonators," *Nat. Photonics* **6**, 480–487 (2012).
27. S. Coen, H. G. Randle, T. Sylvestre, and M. Erkintalo, "Modeling of octave-spanning Kerr frequency combs using a generalized mean-field Lugiato-Lefever model," *Opt. Lett.* **38**(1), 37–39 (2013).
28. V. Ilchenko and M. Gorodetskii, "Thermal nonlinear effects in optical whispering gallery microresonators," *Laser Phys.* **2**, 1004–1009 (1992).
29. <https://www.mathworks.com/help/matlab/ordinary-differential-equations.html>
30. S. B. Papp, P. Del'Haye, and S. A. Diddams, "Parametric seeding of a microresonator optical frequency comb," *Opt. Express* **21**(15), 17615–17624 (2013).
31. D. V. Strekalov and N. Yu, "Generation of optical combs in a whispering gallery mode resonator from a bichromatic pump," *Phys. Rev. A* **79**, 041805 (2009).
32. W. Wang, S. T. Chu, B. E. Little, A. Pasquazi, Y. Wang, L. Wang, W. Zhang, L. Wang, X. Hu, G. Wang, H. Hu, Y. Su, F. Li, Y. Liu, and W. Zhao, "Dual-pump Kerr micro-cavity optical frequency comb with varying FSR spacing," *Sci. Rep.* **6**, 28501 (2016).
33. Y. Liu, Y. Xuan, X. Xue, P.-H. Wang, S. Chen, A. J. Metcalf, J. Wang, D. E. Leaird, M. Qi, and A. M. Weiner, "Investigation of mode coupling in normal-dispersion silicon nitride microresonators for Kerr frequency comb generation," *Optica* **1**, 137–144 (2014).

## 1. Introduction

Optical frequency combs (OFCs), combining thousands of ultrasharp laser lines over a wide frequency spectrum, have enabled ultrashort laser pulses for important applications in optical metrology [1], precision spectroscopy [2], microwave generation [3,4], and optical clock [5]. Traditional OFCs based on mode-locked femtosecond laser technology such as Ti:sapphire solid state lasers or Er/Yb doped fiber lasers, are bulky and lack robustness. Recent advances of OFCs based on the nonlinear Kerr effect in microcavities provide a viable approach to compact and stable comb generations [6–9]. Unlike frequency combs in conventional optical gain media, such OFCs in microcavities rely on the Kerr enabled four wave mixing (FWM) to provide parametric gain. However, other nonlinear processes simultaneously occur and complicate the comb generation (e.g., Raman lasing [10,11], Brillouin scattering [12,13], modulation instability [14], soliton [15–18]). These close-related nonlinear effects can be as important as the original FWM gain in regulating comb generation. For example, in a

traditional laser, gain saturation nonlinearity, the main mechanism limiting multimode lasing, can induce laser spiking which led to the inception of mode-locked lasers later on [19]. Therefore, these Kerr-related nonlinear processes such as soliton are expected to play a crucial role in exploring the on-chip possibility of mode-locked lasers [17,18] rather than an off-chip approach [20].

In this work, we experimentally observe transient nonlinear dynamics, i.e., gain spiking and nonlinear beating, during OFC formation by FWM inside a whispering-gallery mode (WGM) microcavity. We show that gain spiking forms when nonlinear phase modulation plays a major role in the combs' self-detuning from nearby cavity resonances, effectively regulating gain and loss balance for each comb line. This self-stabilization is crucial in the cavity-enhanced gain process, especially in the transient regime. Moreover, this nonlinear phase modulation can also lead to nonlinear beating between an external probe and comb lines, which further verifies its stabilization feature. Such a nonlinear phase modulation may be the foundation for asymmetric comb generation. The current findings may uncover the importance of Kerr-related nonlinearities during OFC generation besides the FWM gain, and we also expect them to be beneficial for future applications in ultrafast optics, wide spectrum generation and ultra-precision metrology on a compact platform.

## 2. Theoretical model

OFCs inside a WGM microcavity arise from Kerr-enabled FWMs: this cavity-enhanced parametric process converts two incoming pump photons into one "signal" and another "idler" as shown in Fig. 1(a) and 1(b). When the intensities of the generated photons build up, they can successively cascade into next generations of photon pairs to form the comb. In the meantime, strict phase matching conditions must be met to fulfill the requirement of momentum conservation. However, such phase matching conditions contain not only linear factors, such as mode dispersion and material dispersion [21], but also nonlinear ones. The most influential ones are the pump-induced self-phase modulation (SPM) and cross-phase modulation (XPM) between signals and idlers [9, 22]. These nonlinear phase modulations (NPMs, including SPM and XPM) effectively alter the effective path lengths photons undergo inside the cavity and hence, also shift their resonances [Fig. 1(c)]. These processes, highly sensitive to pump' intensity, leave the narrow cavity enhanced gains fluctuating around their threshold levels against the cavity losses, which makes OFCs unstable. Similar situations occur in lasers where nonlinear gain saturation can cause the instability of laser operation, where spiking or relaxation oscillations dominate the transient regime [19]. Thus, a properly designed frequency locking mechanism is required to ensure stable OFC generation, e.g., thermal locking or PDH locking [23,24]. Moreover, as the pump power increase, the successive generation of signals and idlers in comb lines start to trigger SPMs and XPMs to each other, limiting further expansion of the OFC, or initiating a new family of comb lines of their own [4]. The latter process leads to gain competition between different comb families, and much like mode competitions in multimode lasers. It also might contribute for the low frequency RF beat noise in OFCs [25,26]. Although the effects of NPMs have been incorporated in the full theoretical model e.g. Lugiato–Lefever equation of OFCs [27], the exact function of NPMs, especially during the transient regime is yet fully investigated.

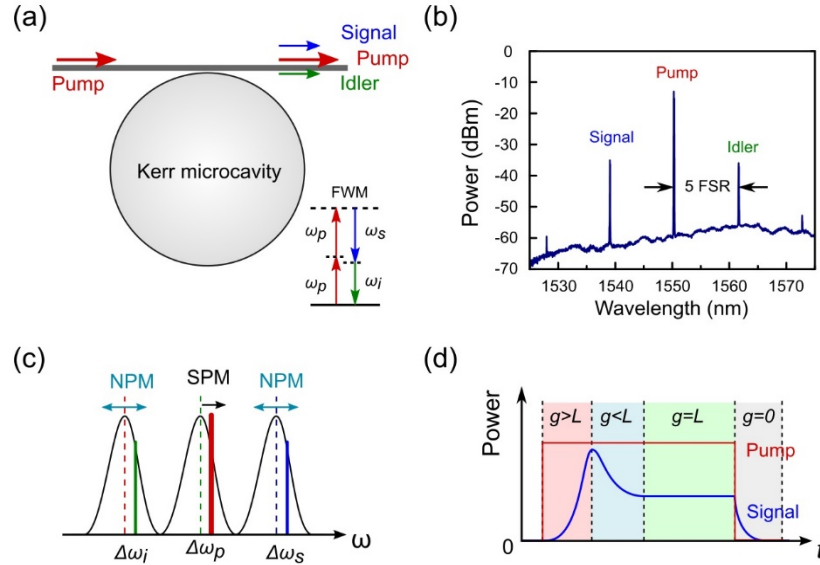


Fig. 1. Illustrations of nonlinear phase modulations and gain spiking during Kerr frequency comb generation in a WGM resonator. (a) OFCs in a taper fiber coupled silica microsphere cavity. (b) Experimentally observed frequency comb spectrum. The pump wavelength is 1550.60 nm. (c) Self-detuning mechanisms from nearby cavity resonances caused by nonlinear phase modulations. They effectively regulate gain and loss balance for comb lines. (d) Schematic illustration of the transient dynamics of OFC generation, showing different regimes of cavity-enhanced gain vs. loss.

More physical insights can be gained from the coupled rate Eqs. (1) and (2) that govern the parametric FWM processes during OFC generation in microresonators. Here the externally injected strong pump  $A_p$  is converted to signal and idler beams through degenerate FWM once the parametric gain is above the threshold set by the cavity decay/loss  $\kappa$ . The frequencies of these three beams satisfy  $2\omega_p = \omega_s + \omega_i$  as required by energy conservation. Meanwhile, the detuning  $\Delta\omega$  of each from its corresponding cavity resonance is adjusted to maintain the phase matching condition. However, this process is complicated by the extra nonlinear phase terms, e.g., SPM and XPM. Previously, the focus of discussion about these NPMs was on XPMs from the pump, since the pump beam is more intense than the signal and the idler. For example, it was found that the pump needs to be blue-detuned from the central cavity resonance during the thermal locking process to overcome the extra nonlinear phase perturbation from the pump's XPM [23]. Here with the growing intensities of cascading signals and idlers, the NPMs of signals and idlers also become influential and can no longer be neglected:

$$\frac{dA_s}{dt} = (-\kappa + i\Delta\omega_s)A_s + \sqrt{2\kappa_e}A_s^{in} + i\gamma \left( \underbrace{A_s|A_s|^2}_{SPM} + 2\underbrace{A_s|A_p|^2}_{XPM} + 2\underbrace{A_s|A_i|^2}_{XPM} + \underbrace{A_pA_pA_i^*}_{FWM} \right), \quad (1)$$

$$\frac{dA_i}{dt} = (-\kappa + i\Delta\omega_i)A_i + i\gamma \left( \underbrace{A_i|A_i|^2}_{SPM} + 2\underbrace{A_i|A_p|^2}_{XPM} + 2\underbrace{A_i|A_s|^2}_{XPM} + \underbrace{A_pA_pA_s^*}_{FWM} \right). \quad (2)$$

Here,  $A$  is the normalized amplitude of a resonator mode.  $\kappa$  denotes the cavity decay rate, including intrinsic ( $\kappa_0$ ) and coupling ( $\kappa_c$ ) loss.  $\Delta\omega$  is the frequency detuning of the wave with respect to its corresponding cavity resonance. And  $\gamma$  is the nonlinear coefficient.

Another key argument to support the existence of signals and idlers' NPMs lies in the steady state analysis of OFCs. To reach the delicate balance between parametric gain and cavity loss for many comb lines, NPMs play an important part in detuning these comb lines from their cavity resonances, fulfilling both energy and momentum conservations for FWMs. However, nonlinear phase corrections from pump are not enough to regulate all the comb lines simultaneously; NPMs from each comb line must participate in the process. OFC lines grow from their initial zero values when their parametric gains are stronger than their cavity loss and a steady state is reached when gains and losses become balanced. This variable gain for each comb line must depend on the comb line's own intensity, which helps stabilizing OFC generation. A similar process occurs in a laser. For example, a single mode laser at the threshold indicates the balance of the laser gain and the cavity loss. A moderate increase of gain will not lead to a second lasing mode. Instead, nonlinear gain saturation or nonlinear detuning from the cavity resonance ensures the rebalancing of gain and loss, which maintains single mode operation.

### 3. Experiment and discussion

To separate the NPMs coming from the pump and that of signals' and idlers' is a challenging task. We achieve the goal experimentally by temporally modulating the pump beam and observing the transient dynamics during OFC' formation near the threshold of parametric oscillations. Here the pump beam at 1550 nm wavelength is thermally locked to a high-Q ( $\sim 10^8$ ) resonance in a silica microsphere cavity with  $\sim 250$   $\mu\text{m}$  diameter (Free spectral range  $\approx 2.2$  nm), using a taper fiber. A relatively low pump power of 5 mW is used to generate OFC with only five comb lines for simplicity [see Fig. 1(b)]. The pump laser is temporally modulated using a square wave at a repetition rate of 100 kHz and 90% duty ratio, which ensures the thermal stability and allows us to monitor the transient dynamics at the same time. Here the rising/falling edge of the square wave function is set around 5 ns, much smaller the cavity ring down  $\sim 100$  ns given  $Q \approx 10^8$ . Meanwhile, the repetition rate of 100 kHz is also carefully chosen to observe nonlinear dynamics at microsecond scale while minimizing thermal effects [28]. Figure 2(a) shows a key finding of this work: the NPMs help stabilizing OFC formation in the transient regime. By tuning the pump beam towards the central resonance, the gated parametric gain in FWM gradually increases in each panel of Fig. 2(a) through cavity enhancement effect. In this manner, we can obtain a controllable quasi-stable gain while avoiding other unstable problems, e.g., loss of thermal locking of the pump. As shown in panels II and III in Fig. 2(a), the main signal line starts to grow right after the gated gain, gradually reaching a steady-state level and stabilizing itself for a relatively small gain. For a larger gain, the signal rapidly rises and quickly falls right afterwards, forming a "spike" as shown by panels V and VI in Fig. 2(a). The same effect is observed on the idler side simultaneously (not shown). These self-evolving processes are a result of NPMs shown in Fig. 1(d): Initially, the FWM parametric gains exceed the cavity losses, generating signals and idlers. The growing powers of signals and idlers effectively detune them from the corresponding resonances through NPMs, reducing their gains until the steady state level is reached, where the balanced between gain and loss is established. A similar process takes place in a laser, where nonlinear gain saturation provides the feedback mechanism during gain spiking [19]. Because the pump intensity (and the XPMs it imposes on the signal and idler) is a constant during this process, the temporal variation of gain must originate from the variations of the signal and idler intensities, i.e., due to their SPMs and the XPMs between themselves. This understanding is supported by our numerical simulations [Fig. 2(b)] based on solving coupled equations of Eq. (1) and (2) by Matlab's ODE package [29], where this

self-stabilization and spiking effect only present themselves if the NPM terms from the signal and the idler are considered. The extra oscillation in the simulation may due to lack of higher bandwidth photo-detection in our experiment, which requires further studies.

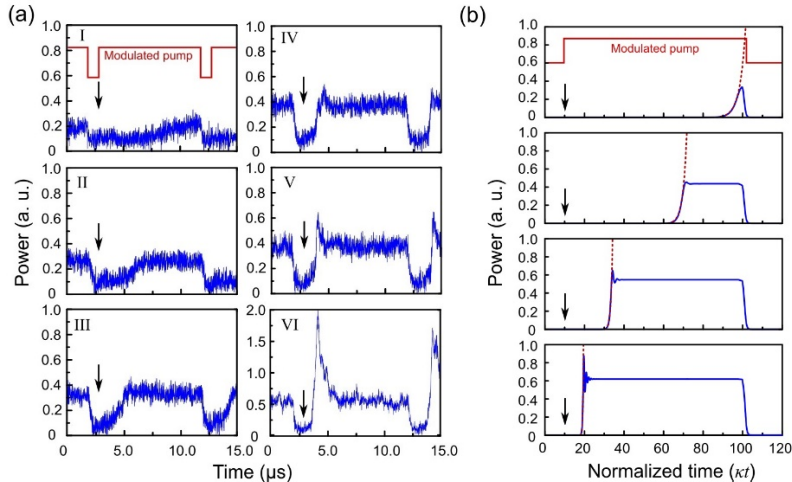


Fig. 2. Experimental observations of gain spiking of OFCs. (a) Time traces of the filtered signal side-band around 1539nm with respect to a traveling gated pump (inferred red curves). From panel I to VI, as the pump is tuned towards the resonance center gradually enhancing the FWM gain, the rising edge of the signal tends to steepen, and finally lead to spiking formation in the large gain regime. The arrows show the turn-on points of the pump. (b) Numerical simulations of signal dynamics with (blue lines) and without (red dot) NPMs, with increasing FWM gain from top to bottom. The XPM of the pump, assumed to be a constant in each panel, is excluded from the simulations.

As shown above, NPMs due to the signal and idler intensities are crucial in stabilizing OFCs during their onset. Next we probe XPMs between signals and idlers. Since they have almost identical intensities inside the microcavity due to the energy conservation of FWMs, we must introduce an external perturbation to break this symmetry. Here in our experiment, a second external coherent laser is injected to a stable OFC (constant pump) similar to the seeding method in OFCs [30], however, in order to demonstrate the XPMs, we have to sweep the probe laser with temporal modulations across the signal comb line marked in Fig. 1(b) to observe XPMs in a transient fashion. Meanwhile, without disturbing the original OFCs, the power of the seeded laser is fixed below 1/100 of the original pump's during the sweeping, which is comparable to the power of the signal output from the taper fiber. As the external laser is tuned across the signal line, these two coherent beams experience chirped beating between themselves, which is purely *linear effect*. For the corresponding idler, not much intensity fluctuation is observed when the external probe is small, except at the center of idler line where an intensity spike appears [Fig. 3(a)], indicating extra parametric gain due to the external probe. We note that the output intensity of the signal depends on the relative phase between the signal and the probe, and in this figure they appear to be  $\pi$  out of phase and result in an intensity dip when the probe is right at the signal line. More interestingly, when the pump power increases, chirped oscillations appear on both wings of central idler line as well. This is because the external probe now induces its own idler through optical parametric amplification (OPA) much like double-pumped OFCs [31], which linearly interferes with the original idler comb line. However, such interference beatings diminish in both signal and idler when the probe frequency is close to the original signal line, implying that two parametric processes, i.e. the OFC and the OPA of the probe, have emerged into a single process. The width of this regime is an effectively measurement of OFC's gain width, proportional to the pump power as shown in [9]. Such a beating-free regime indicates that the

signal frequency of OFC is tunable within its gain width and governed by the frequency of the probe. During this process NPMs of the pump is maintained at a constant level, and hence NPMs of the signal and idler, especially the XPM between them, must participate to regulate nonlinear phases of the signal and idler lines. As we show in the following section, this regime provides a unique platform to study the effect of XPMs via the control of the signal. This nonlinear beating phenomena should also appear and play an important role in OFCs with multiple pumps [31,32].

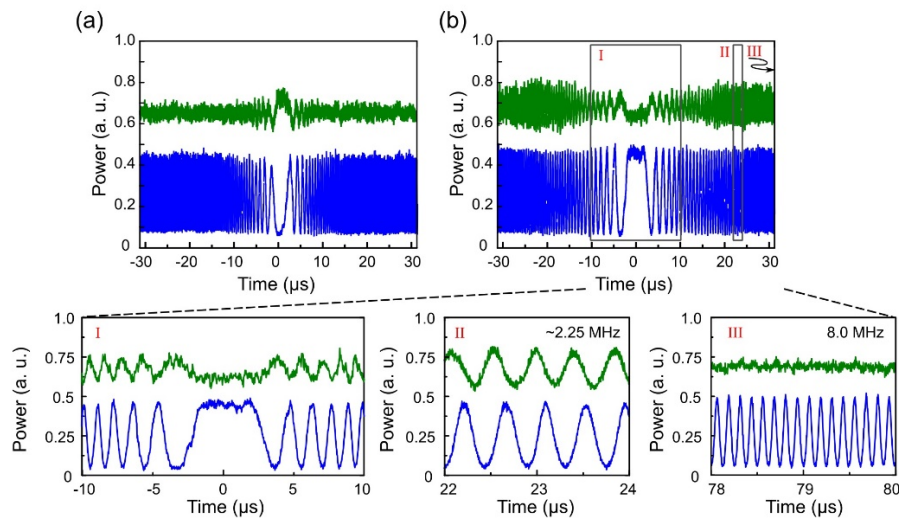


Fig. 3. Nonlinear optical beating of OFC and an external probe in the microcavity. The beating of signal (linear beat) was achieved by sweeping a probe across the signal comb line at 1539.3 nm. The pump is fixed at 1550.6 nm with a constant power during the sweeping, and the OFC is the same as Fig. 1b before the probe is introduced. As the pump power increases from (a) to (b), the coalescence of the signal and the probe (blue line) is clear as their frequencies become close. In (b) a chirped beat note was observed at the idler frequency (1562.0 nm; green line), which vanished nonlinearly on resonance (panel I). The scan speed is 0.1 MHz/ $\mu$ s.

To directly demonstrate the effect of XPMs, we set the external probe in the beating-free regime and near the signal line of the OFC. We then again adopt the modulation technique by modulating the probe laser to observe OFC's transient behaviors. As shown in Fig. 4, the variation of the idler intensity depends on the modulation depth of the probe. When the inner-cavity signal modulation is small, the idler's waveform is dramatically distorted from a square wave, behaving like a slow rise-and-fall in Fig. 4(a). In contrast, with increasing modulation depth of the inner-cavity signal (decreasing in signal output), such rising/falling edges become sharper and more instant, almost following the signal's square waveform. The mechanism behind this behavior is very similar to the gain detuning processes with the pump modulation mentioned above and shown in Fig. 2: the XPM from the signal causes an effective detuning of the idler, breaking the balance of the gain and the loss established before the modulation of the signal. Right after the sudden change of rising/falling edges of signal, the idler tends to re-stabilize itself after this sudden detuning caused by XPM. As can be easily understood, a large modulation of the signal will lead to a wide imbalance between idler's gain and loss, giving rise to a quick re-stabilization in Fig. 4(c). These observed dynamics has also been consistent with numerical simulations in Fig. 4(d)-4(f) with increasing FWM gains. The observation here of asynchronous or hysteresis behaviors between the signal and idler may help understand a long-standing issue in OFCs, i.e. asymmetrical combs, which was attributed to linear factors such as loss and dispersion [33]. Here, we believe such nonlinear NPMs may also play an important role in generating

asymmetry OFCs, which may also open up a new avenue in all-optical signal processing such as non-reciprocal multiplexing.

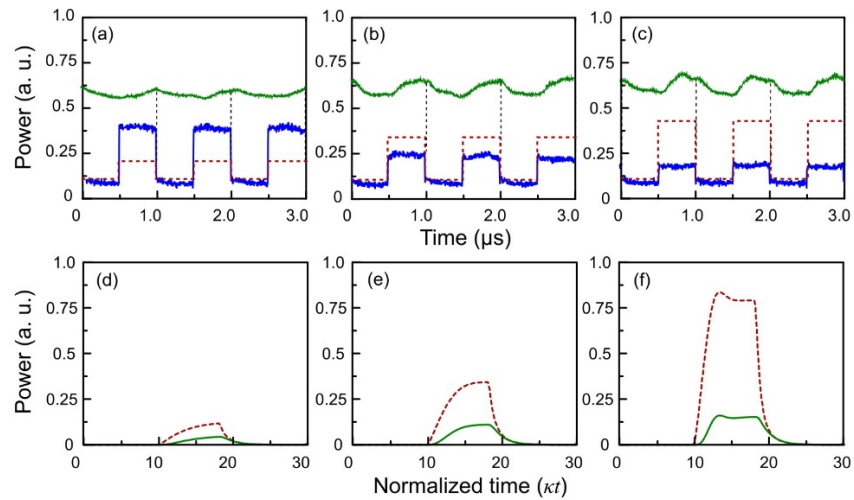


Fig. 4. NPMs between the signal and idler of OFCs. (a-c) experimental observations, (d-f) numerical simulations of idler re-stabilization through XPMs of signal modulation. The green, blue, red curves are for idler, signal output, inner-cavity signal, respectively. Note that the inner-cavity signal modulation is difficult to obtain experimentally in the transient regime, the measured signal outputs mix with original come line signal and the external probe. Here the red curves in (a-c) are inferred from the signal output i.e. total power of the external probe and signal minus the measured signal output.

#### 4. Conclusions

In conclusion, we have demonstrated transient nonlinear dynamics during the onset formation of OFCs inside the Kerr microcavity. We showed that gain spiking forms due to NPMs and causes comb lines' self-detuning from nearby cavity resonances, effectively regulating gain and loss balance for each comb line, which is one key mechanism to stabilize OFCs. Moreover, we have observed nonlinear beating by injecting an external probe to examine nonlinear XPM between an external probe and comb lines. These nonlinear transient dynamics reveal the importance of Kerr-related nonlinearities during OFC generation besides the FWM gain. It would be beneficial for future applications in mode-locking comb and tunable comb generation on a compact platform.

#### Funding

National Key Research and Development Program (Grant No. 2016YFA0302500); National Natural Science Foundation of China (Grant No. 11674228 No. 11304201, No. 61475100); National 1000-plan Program (Youth); Shanghai Scientific Innovation Program (Grant No. 14JC1402900); Shanghai Scientific Innovation Program for International Collaboration (Grant No. 15220721400); PSC-CUNY Cycle 48 seed funding.